Raman study of photoinduced chain-fragment ordering in $GdBa_2Cu_3O_x$ thin films

A. Fainstein, P. Etchegoin, and J. Guimpel*
Centro Atómico Bariloche, Comisión Nacional de Energía Atómica, 8400 S. C. de Bariloche, R.N., Argentina
(Received 1 June 1998)

Raman scattering experiments on oxygen deficient $GdBa_2Cu_3O_x$ thin films ($x=6.53$, 6.7, 6.8, and 6.93) as a function of photoexcitation and annealing induced oxygen disorder are presented. Raman lines, unambiguously assigned to copper and oxygen vibrations involving atoms at the end of Cu-O chains, are used as markers for the existence of short chain fragments. The dynamics of chain conjunction and fragmentation was monitored by the peak intensity dependences with photoexcitation time and annealing temperature. These results demonstrate the presence of photoassisted oxygen ordering in these high-T_c superconductors, and give definitive support for its ultimate role in the phenomena of persistent photoconductivity and photoinduced superconductivity. [S0163-1829(98)04037-5]

I. MOTIVATION

The existence of persistent photoconductivity (PPC) (Ref. 1) and photoinduced superconductivity (PS) (Ref. 2) in oxygen deficient $YBa_2Cu_3O_x$ thin-films was established shortly after the discovery of high-temperature superconductivity. A wealth of transport (Hall and electrical resistivity)[1–4] and spectroscopic (excitation efficiency, infrared absorption, and luminescence)[3,5–7] experiments have been reported showing that illumination with visible[3] or UV light[7] produces an increase in the conductivity and the superconducting critical temperature of the material. These changes are metastable if the sample is kept at temperatures below 250 K, and relax back to the equilibrium state at higher temperatures. The potentiality of photoinduced superconductivity has been recently demonstrated by the nanoscale drawing of superconducting circuits by local illumination with a scanning near field microscope.[8] Notwithstanding the development of the field, the microscopic process by which illumination generates such long lived physical changes is unclear. In fact, though it is well established that the phenomena are due to photoinduced doping of the CuO_2 planes by electron-hole pair excitation, the electron trapping mechanism is still under debate.

Basically, two models are cited in the literature to explain the origin of these metastable states, namely, photoassisted oxygen ordering[4] and trapping at oxygen vacancies.[7,9] Arguments based on experimental evidence have been brought up apparently supporting both of them. In the first model, the photoexcitation is thought to induce oxygen ordering into longer chains, which are well known to constitute better hole dopants (and hence electron traps) than shorter fragments.[10] Both, oxygen ordering and photoinduced conductivity produce similar behaviors for the relaxation time scales and T_c changes[2,4] and point out a connection between the two physical processes. Further support for this scenario is found in the contraction of the *c* axis observed both with oxygen ordering (due to an induced orthorhombicity) and illumination.[4] In the second model, on the other hand, the photoexcited electron is trapped into an oxygen vacancy in the Cu-O chain layer, leading to a local distortion that acts as a barrier for recombination. Arguments raised in favor of this latter mechanism, common also to other insulating and semiconducting materials, are the existence of a peak in the photoexcitation eficiency in the UV spectral range,[7] the correlation between the spectral efficiency curve[3] and the photoluminescence spectra,[6] and the existence of a monotonic behavior for the $\Delta\sigma/\sigma$ vs oxygen content curve. None of these experiments, however, give direct insight into the atomic rearrangements taking place during photoexcitation. In this paper we present Raman scattering experiments in $GdBa_2Cu_3O_x$ thin films that provide such microscopic probe. These experiments rely on the recent unambiguous identification of Raman lines that are due to vibrations at the end of Cu-O fragments, which can be used as markers for the existence of short chains.[11]

Raman scattering has been extensively used to study the vibrational, electronic, and magnetic properties of high-temperature superconductors.[12,13] Relevant experiments have measured the superconducting gap, determined the symmetry of the condensed state, or have been used to study the electronic structure of the insulating and superconducting phases. The phonon scattering spectra, moreover, have been used to verify isotope substitution, determine the presence of impurity phases and twins, or estimate electron-phonon coupling constants. Most of the predicted Raman allowed phonon modes have been observed,[12–15] and their resonant behavior determined.[16,17] However, the use of Raman scattering to study the presence and ordering of chain fragments in oxygen deficient $YBa_2Cu_3O_x$ has been hampered by the fact that both the copper and oxygen chain atoms occupy inversion centers and thus do not participate in Raman allowed modes. Oxygen ordering during annealing and evidence for the coexistence of ortho-I, ortho-II, and tetragonal microstructures has been monitored through Raman scattering in a rather indirect way by analyzing the line shape of the Raman allowed band due to the *neighbor* apical-oxygen vibrations.[18,19] The recent remarkable micro-Raman experiments of isotope substitution during local laser annealing by Ivanov *et al.*[11] constitute a breakthrough to this situation: by observing the change of the mode frequency after a site selective $^{18}O \leftrightarrow {}^{16}O$ substitution they were able to unambiguously assign two Raman bands located around 248 cm^{-1} and 596 cm^{-1} to vibrations of copper and oxygen atoms, respec-

tively, at the end of short chain fragments. These modes become Raman active due to loss of inversion symmetry of the atomic sites, and are thus forbidden for infinite (or very long) chains. The assignment of these ''defect'' modes is consistent with an earlier suggestion of Wake *et al.*[20] Subsequent detailed work by Iliev *et al.*[21] has exploited these and other features of the Raman spectra to probe the transformation of the local oxygen arrangements (microdomains) with changes of oxygen content upon laser annealing. We have used these spectral lines to follow the evolution of the chain-fragment distribution during thermal treatment (annealing above room temperatures at *constant* oxygen content) and illumination with laser light. These results provide evidence for the conjunction of short Cu-O fragments into longer chains with photoexcitation, and confirm that long fragments break into shorter ones with annealing at increasing temperatures.

The paper is organized as follows. In Sec. II we describe the samples, experimental setup, and procedure used to measure the Raman spectra during annealing and photoexcitation. Section III presents our results and discussion. The conclusions are drawn in Sec. IV.

II. SAMPLES AND EXPERIMENT

The $GdBa_2Cu_3O_x$ thin films were grown by dc magnetron sputtering from a stoichiometric target in the parallel off-axis configuration.[22] Film deposition was done in an $Ar(90\%)/O_2(10\%)$ mixture at a total pressure of 300 mbar. The substrate temperature was controlled at 760 °C during this stage. After deposition, the films were cooled down to 450 °C and oxygenated for 1 h at 100 Torr of pure O_2. The film thicknesses are around 2000 Å for a two hour deposition period. The x-ray diffraction spectra show (001) oriented growth over the single crystalline (100) MgO substrates. The as-grown films show linear metallic resistivity behavior, and T_c's of 85–90 K, with transition widths of 2 K. The oxygen content of the samples was adjusted in a controlled manner using the isostoichiometry line annealing method.[23] Four samples, with nominal oxygen content $x=6.53$, 6.7, 6.8, and 6.93 (''fully'' oxygenated), respectively, were studied. Prior to any Raman measurements the samples were left to anneal several days at room temperature (292 K). Films prepared under exactly the same conditions were used in the PPC experiments reported in Ref. 24.

Raman spectra were collected with a triple Jobin-Yvon T64000 spectrometer working in subtractive mode, and detected with a liquid N_2-cooled charge coupled device camera. The 514.5 nm line of an Ar-ion laser was used for excitation in a backscattering geometry with parallel incident and scattered polarization $[z(x,x)\bar{z}$ configuration in Porto's notation]. Laser powers ranging from 1 to 50 mW were focussed to a (relatively large) circular spot of ≈ 100 μm diameter. A closed cycle refrigerator equipped with an optical quartz window was used for controlled temperature experiments, while a liquid-N_2 cold finger cryostat was preferred when fast cooling rates were required (a quench from room temperature to 80 K takes approximately five minutes in this latter system). Experiments on each sample consisted of the three following stages: (i) a quench from room temperatures down to 80 K and collection of Raman spectra every 10 min during 5 Hs of continuous illumination, (ii) a rapid heat up to room temperature, followed by Raman data collection (again every 10 min) during the slow heating of the sample up to 375 K (typically a 2.5 Hs ramp and 0.5 Hs annealing at 375 K), and (iii) a quench from 375 down to 80 K, and collection of Raman spectra during 5 Hs as in stage (i). For each stage the laser spot was focused onto a new nonilluminated part of the sample. During the illumination periods the light source for the photoexcitation was the same laser line used for Raman data collection. The laser power, wavelength, and integration time were selected so as to have good quality spectra and, at the same time, a continuous smooth variation of the studied spectral features. This means that during the annealing in stage (ii), the thermal treatment coexists inseparably with photoexcitation. This is not of great concern for the higher temperatures (335–375 K) where the thermal induced disorder is so fast that the sample reaches almost instantly a stationary state.[24] For the lower temperatures (295–335 K), however, the spectra are slightly different if they are taken during the warming ramp, or after a long annealing at fixed temperature. In all cases the sample temperature and laser power density were such that changes of oxygen content due to in or out diffusion (as in Refs. 11 and 21) could be ruled out.

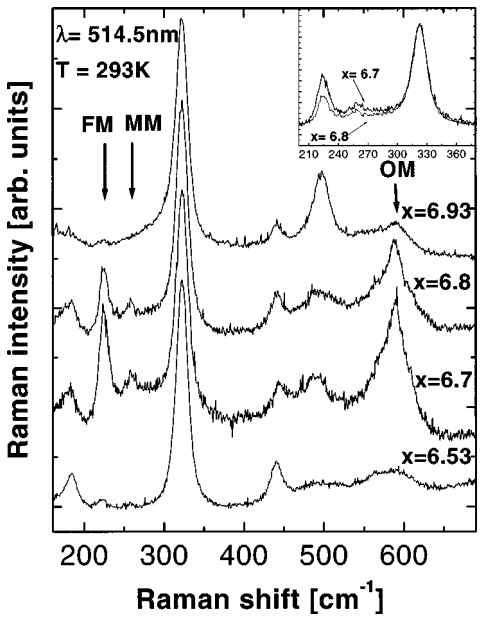

FIG. 1. Room temperature phonon Raman spectra of $GdBa_2Cu_3O_x$ thin films with varying oxygen content. The vertical arrows denote the Raman ''forbidden'' modes assigned to copper (FM and MM) and oxygen (OM) vibrations involving atoms at the end of Cu-O chains. These modes become allowed in *finite* chain fragments due to the lack of inversion symmetry. Note that these lines are not observed for $x=6.53$ and $x=6.93$ as expected from the infinitely long chains existing in the ortho-I and ortho-II structures formed in the basal planes at these oxygen contents. The inset compares the data at intermediate oxygen contents in the spectral region corresponding to copper-related vibrations.

III. RESULTS AND DISCUSSION

In Fig. 1 Raman spectra taken at room temperature (292 K) for the four studied samples are shown. Several phonon

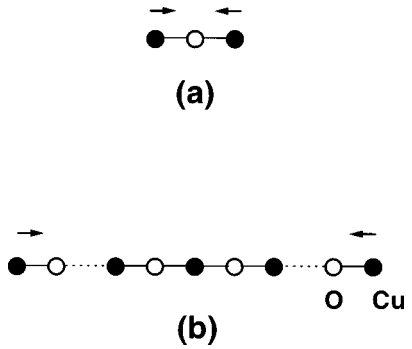

FIG. 2. Scheme of the Raman active modes involving displacement of copper atoms at the end of Cu-O-Cu ''monomers'' (a) and chain fragments (b). These modes are labeled in the text as MM and FM, respectively. See Ivanov *et al.* (Ref. 11) for a detailed discussion of the symmetry and assignment of the Raman modes due to vibrations involving copper and oxygen atoms at the end of chain fragments.

lines due to Raman-active (z)-polarized A_g symmetry modes are observed at 160 cm^{-1} (CuO_2-plane copper in-phase mode), 330 cm^{-1} (CuO_2-plane oxygen out-of-phase mode), 435 cm^{-1} (CuO_2-plane oxygen in-phase mode), and 500 cm^{-1} (apycal oxygen mode). Besides these Raman-allowed bands many additonal spectral features appear usually in oxygen deficient $YBa_2Cu_3O_x$ samples, due to local changes of the atomic environment resulting in activation of otherwise Raman-forbidden modes.[12–15] Of these additional lines, two at 248 and 596 cm^{-1} were recently unambiguously assigned[11] to A_g-symmetry stretching vibrations of copper and oxygen atoms, respectively, at the end of short chain fragments (see the scheme in Fig. 2). This identification was accomplished by studying the evolution of the phonon spectra of *tetragonal* $YBa_2Cu_3{}^{18}O_{6.2}$ microcrystals after a site selective isotopic substitution with ^{16}O. This assignment is also consistent with the copper and oxygen Raman-*allowed* vibrations of the *double* Cu-O chains of the ''124'' $YBa_2Cu_4O_8$ compound,[25] observed around 250 and 605 cm^{-1}, respectively. We identify these vibrations with

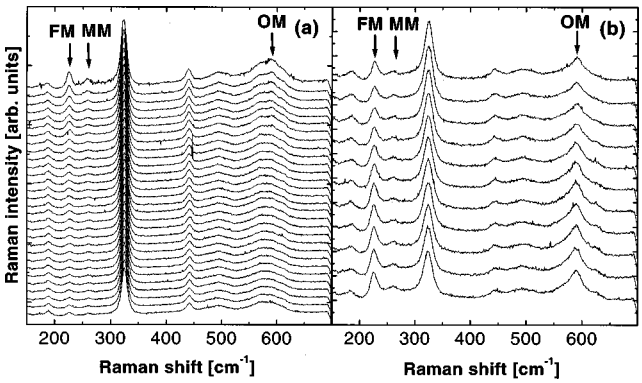

FIG. 3. Raman spectra continuously taken with 10 min integration time for (a) illumination with 50 mW 514.5 nm laser light at 80 K after a rapid (5 min) quench from room temperatures and (b) annealing with increasing temperature from 295 to 375 K. The time increases from top to bottom. The spectra correspond to the sample with oxygen content $x=6.8$. The vertical arrows denote the studied Raman modes.

the strong spectral features observed at 225, 260, and 595 cm^{-1} (marked with arrows in Fig. 1), present for the samples with intermediate oxygen content ($x=6.7$ and $x=6.8$). The fact that only residual features are observed at these frequencies for the samples with $x=6.53$ and $x=6.93$ confirms these assignments: the equilibrium state at these oxygen contents corresponds to the ortho-I and ortho-II structures, respectively, characterized both for the presence of infinitely long (and hence Raman inactive) Cu-O chains.[10] The fact that two lines are observed at 225 and 260 cm^{-1} (and not only one at 248 cm^{-1} as in Ref. 11) is consistent with the data reported for orthorhombic $YBa_2Cu_3O_x$ (see, e.g., Refs. 14, 20, and 21). The possible origin of this difference will be further discussed later. For the time being, we will only consider (as in Ref. 21) that the two lines around 250 cm^{-1} and the line at 595 cm^{-1}, correspond to stretching vibrations of copper and oxygen atoms, respectively, at the end of short chain fragments.

The reason for the activation of these modes can be easily explained in a practical way starting from a bond-polarizability model (BPM) (Ref. 26) for the Raman efficiency as follows (a group theory mode analysis can be found in Ref. 11). In a macroscopic formulation of Raman scattering, the Raman efficiency can be written as $\sigma \propto (\partial\alpha/\partial u)u$. It reflects the *change* of the electronic polarizability α due to the phonon-induced atomic modulation u. The BPM provides a simple way to evaluate σ by postulating that the electronic polarizability can be expressed as a sum of *individual* bond polarizabilities (which are assumed to be independent of the chemical environment). If an atom is located at the inversion center of a Cu-O chain and is displaced along the chain direction, the change of the polarizability of all bonds to one side is exactly compensated by the bonds on the opposite side. When a chain is infinitely long, this cancellation occurs for all atoms. However, for a finite fragment, the displacement due to even modes (respect to the fragment inversion center) involving the atoms at the extremes of the chain is not compensated leading to a finite Raman cross section. Note that for the copper atoms at the end of the fragment the modulation of the strongest first near neighbor Cu-O bond contributes to the Raman efficiency. For the *second* pair of copper atoms, instead, the noncompensation starts only with the third-near-neighbor copper-oxygen bond. This implies that the main part of the observed Raman signal will arise from vibrations of the atoms at the end of the Cu-O fragment. Having realized this, one can see that the intensity of these modes can be used almost as a *counter* of chain fragments. In fact, in order to study the process of chain fragment formation in oxygen deficient $YBa_2Cu_3O_x$, the Raman inactivity of the copper and oxygen atoms in long chains turns out to be of a great advantage. Consider as an example two chain fragments separated by an oxygen vacancy, and nearby a ''monomer,'' consisting of a single oxygen atom bonding two coppers. Any physical process producing the jump of the latter oxygen atom to the vacancy separating the fragments would reduce the Cu-vibration Raman signal to *one third* of the original value. A physical probe sensitive to all the atoms in the chains such as, e.g., infrared absorption,[12,13] would display instead only a subtle change due to the minor effect on the global dielectric susceptibility.

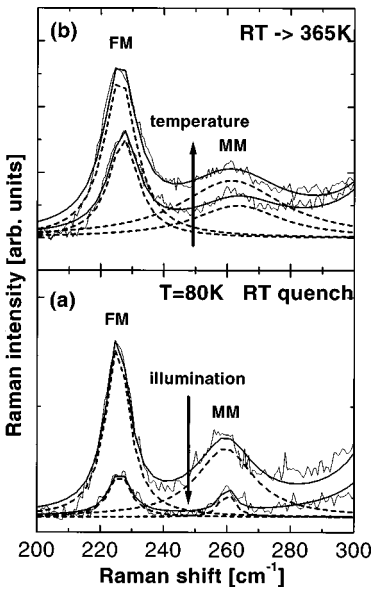

FIG. 4. Examples of the three Lorentzian line fits performed for a quantitative analysis of the spectra. Only the relevant FM and MM lines are shown. The spectra correspond to the first and last curves in Figs. 3(a) and 3(b). The fit to the individual peaks are shown with dashed curves. The thick solid curve corresponds to the full fit, including the Raman allowed mode at 330 cm^{-1} (CuO_2-plane oxygen out-of-phase vibration). The arrows indicate the direction of increasing illumination dose or temperature, respectively. Note the strong optical bleaching of the two lines, and their enhancement with increasing oxygen disorder (annealing temperature). Note also in (a) the photoexcitation induced line narrowing of the MM mode. In the text, the Raman intensity is defined as the integrated area of the fitted Lorentzian peaks.

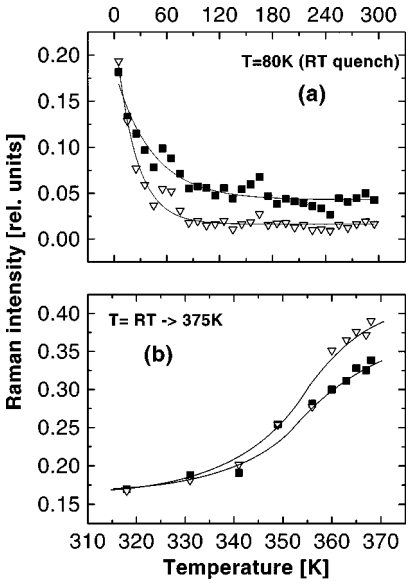

FIG. 5. Raman intensity of the FM (squares) and MM (triangles) peaks, (a) as a function of illumination time with 50 mW 514.5 nm laser light at 80 K after a rapid quench from room temperature and (b) as a function of temperature while heating the sample from room 295 to 375 K. These data correspond to the spectra in Figs. 3(a) and 3(b). The curves in (a) are fits with exponential decays. The time constant is inversely proportional to the laser power density. The curves in (b) are guides to the eye. Note that for the data in (b) a true annealing only occurs for temperatures higher than about 335 K. The temperature ramp is too fast to allow complete oxygen ordering at lower temperatures.

In Fig. 3 we show typical Raman data taken every 10 min, for the sample with $x=6.8$, during illumination at 80 K (a), and while heating up to 375 K (b). Spectra in (a) correspond to stage (i) described above, while spectra in (b) to stage (ii). The data of stage (iii) are qualitatively similar to that in (a). It is evident that the peaks assigned to vibrations at the end of chain fragments (marked with arrows) *decrease* or almost disappear with photoexcitation, while they are *enhanced* with annealing at increasing temperatures. The other phonon lines are basically independent of illumination time or annealing. The peak at 595 cm^{-1} is more or less prominent for the different studied samples or scans. It is, however, always on top of a broad constant featureless band that thwarts its analysis. In what follows we will hence only center our quantitative discussion on the copper vibration modes at 225 cm^{-1} (FM) and 260 cm^{-1} (MM). The reason for the election of these labels will be justified later (FM stands for ''fragment'' mode, MM for ''monomer'' mode). Within our experimental error the peak at 595 cm^{-1} displays basically the same general behavior. We have analyzed the spectra by performing fits with three Lorentzians of the spectral region between 200 and 380 cm^{-1}. Typical fits of the first and last spectra of Figs. 3(a) and 3(b) are shown in Fig. 4. The spectra are reasonably well described by two narrow peaks at 225 and 330 cm^{-1} (not shown), and a broader one centered around 260 cm^{-1}. The latter takes into account not only the contribution of the peak itself, but also a background scattering observed between $\approx$240 and $\approx$290 cm^{-1}, most notable for the shorter illumination time spectrum in Fig. 4(a) and the larger temperature one in 4(b). Note in Fig. 4 the clear optical bleaching and enhancement with increasing temperature of the FM and MM peaks.

Figure 5 shows the Raman intensity of the FM and MM peaks as a function of illumination time, measured at 80 K after a rapid quench from room temperature (a), and as a function of temperature during annealing up to 375 K (b). These curves correspond to the sample with oxygen content $x=6.8$ (spectra shown in Fig. 3). The Raman intensity is defined here as the integrated area of the fitted lorentzian peaks, normalized with respect to the CuO_2-plane oxygen out-of-phase mode at 330 cm^{-1}. This is done to take into account any possible alignment variation during the long integration times. Besides this Raman intensity change, it is apparent from Fig. 4(b) that there is also a photoexcitation induced narrowing of the broader peak centered at 260 cm^{-1} (MM). The linewidth dependence on illumination time of the three fitted peaks is shown in Fig. 6. Several features can be commented on these two last figures: (i) an exponential-like decay with saturation of the intensity of both FM and MM peaks is observed with photoexcitation. We have verified that, as for the PPC (Ref. 1) and the PS (Ref. 2) experiments, the decay times scale inversely with the incident laser power, meaning that the important parameter is the illumination dose. However, the saturation value (around 25% of the first point for this sample) is independent of laser power. At this low temperature any illumination induced changes remain frozen, and only relax back to their equilibrium value above $\approx$250 K. (ii) The normalized intensity of the two peaks in-

creases with increasing sample temperature. Below $\approx 330-340$ K the time scale of the experiment does not allow to reach a stationary state in Fig. 5(b), and the effect is thus partially compensated by simultaneous photoexcitation. (iii) Both the optical bleaching and the annealing enhancement are more pronounced for the MM mode, which almost disappears with photoexcitation. (iv) The linewidth of the FM peak is illumination independent, while the MM peak displays a photoexcitation induced narrowing with an exponential decay behavior.

Point (i) above provides definitive evidence for the conjunction of short Cu-O fragments into longer chains during irradiation with laser light at 514.5 nm. On the other hand, point (ii) confirms the established knowledge that annealing at higher temperatures produces the fragmentation of the longer chains, basically due to the role of the configurational entropy in the free energy of the system.[10] This disordering of the Cu-O chains at constant oxygen content has been previously investigated by Raman scattering through its indirect effect on the line shape of the apycal oxygen mode at 500 cm^{-1}.[18,19] In this context, the contrasted behavior observed with illumination and annealing in Fig. 5 can be taken as a consistency argument for the interpretation of point (i). These two features together bring strong support for the existence of photoassisted oxygen ordering in oxygen deficient $GdBa_2Cu_3O_x$ thin films, and on the role of the latter in the observed persistent photoconductivity and photoinduced superconductivity.[4]

While the above conclusion emerge directly from the data, the understanding of points (iii) and (iv) requires an additional hypotesis on the origin of *two separate* peaks linked to vibrations of copper atoms at the end of chain fragments (FM and MM). We believe that our data can be consistently explained if we assign the higher frequency mode at 260 cm^{-1} to copper stretching vibrations in Cu-O chain *monomers* (MM), while the mode at 225 cm^{-1} would correspond to vibrations of the end copper atoms in longer fragments (FM). We base this tentative assignment on the following two observations: first, both the chain Cu-O bond and the chain-Cu-apycal-oxygen bond are reduced around 1 and 3 %, respectively, when going continuously from $x=7$ (orthorhombic) to $x=6.35$ (tetragonal).[27] The higher frequency of the monomer vibration can be explained if a local order close to the tetragonal structure is assumed around these short and disordered fragments, while an orthorhombic bond length applies for the longer chains. The force constant depends on the third power of the atomic distances,[25] thus explaining the order of magnitude of the observed shift. Such ''incipient orthorhombicity'' effect should be absent in tetragonal $YBa_2Cu_3O_x$: this is consistent with the observation of only one peak in Ref. 11. Second, the Cu-Cu nearest neighbor relative displacement is larger for the monomer vibration than for the longer fragments (see the scheme in Fig. 2): this augments both the stretching force energy and the Coulomb repulsion, shifting the MM mode in the same direction as the bond contraction. Within this interpretation the curves in Fig. 5(a) imply that photoassisted ordering occurs mainly through the displacement of monomer oxygen atoms which incorporate themselves at the end of, or help to bond, larger fragments. In fact, each disappearing monomer is accompained by a reduction of the related Raman signal. On the other hand, only the conjunction of fragments into larger ones should be reflected on the bleaching of the peak at 225 cm^{-1}, but not their slight length increase by the incorporation of a single oxygen atom. This accounts for the major sensitivity of the MM mode with photoexcitation. Figure 5(b) indicates also that the creation of monomers is the preferred path for entropy increase with annealing. The monomer mode frequency should be more sensitive to the local order (the nearby presence of chain fragments, or individual oxygen atoms in orthogonal Cu-O bonds), through its impact on the Cu-O bond lengths. In fact, a distribution of frequencies may be expected, that shrinks with oxygen ordering in the Cu-O planes. This scenario is consistent with the linewidth dependence with illumination displayed by this mode in Fig. 6.

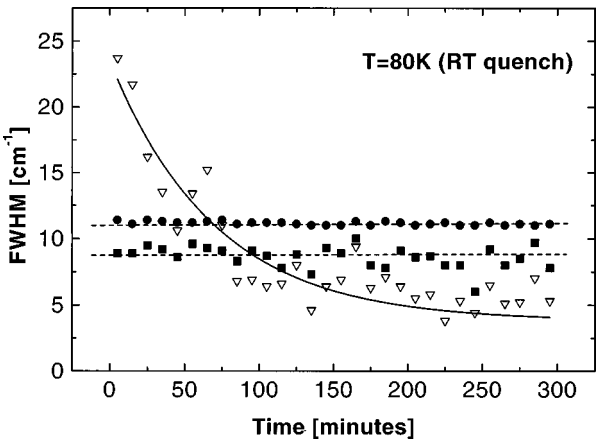

FIG. 6. Linewidth (defined as the full width at half maximum of the fitted Lorentzian lines) of the FM (squares), MM (triangles), and 330 cm^{-1} (circles) peaks as a function of illumination time with 50 mW 514.5 nm laser light at 80 K after a rapid quench from room temperature. The data correspond to the spectra in Fig. 3(a). Note the photoexcitation induced narrowing of the MM line. We tentatively assign this latter mode to the vibration of copper atoms in Cu-O-Cu monomers, and the FM mode to copper vibrations at the end of larger chain fragments (see the text for details). The solid curve is a fit with an exponential decay. The dashed lines are guides to the eye.

Although the physical mechanism involved in photoexcitation and oxygen disorder by annealing is the same, as we have demonstrated here, resistivity studies in $GdBa_2Cu_3O_x$ thin films show that they behave as noninteracting from the point of view of persistent photoconductivity.[24] One consequence is that they *do not* cancel out: the final state obtained by photoexcitation is not the same for initial states characterized by a different oxygen order.[28] This nonadditivity of photoexcitation and annealing induced oxygen disorder is also found in our Raman data. In fact, a systematic shift towards a larger number of chain fragments, that cannot be cancelled by photoexcitation, is observed when the sample is quenched from 375 K as compared with room temperature. This is shown in Fig. 7 for the FM peak measured in the sample with composition $x=6.7$. The two curves shown correspond to the experiments (i) and (iii) described in Sec. II. Within our experimental resolution the MM peak displays basically the same behavior as the FM mode. We note that for the sample with $x=6.8$ the two experiments could not be distinguished within our experimental error.

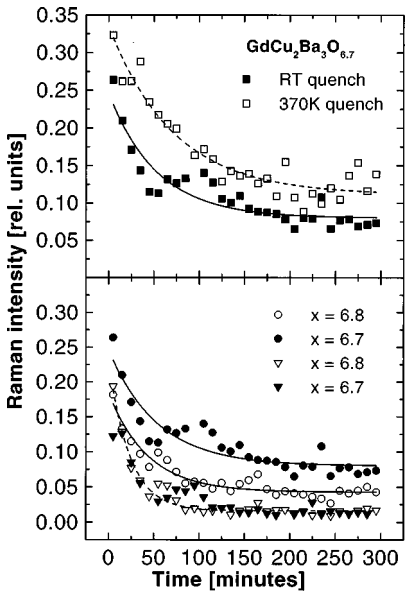

FIG. 7. (a) Illumination time dependence of the Raman intensity of the FM mode after a rapid quench to 80 from 295 K (solid squares) and from 375 K (open symbols). Note the systematic shift to larger values after a quench from the higher temperature, indicating the presence of a larger number of chain fragments. The MM mode displays, within our experimental resolution, the same behavior. The curves are fits to the data with exponential decays. (b) Comparison of the illumination dose dependence of the FM (circles) and MM (triangles) Raman peaks for the two studied samples $x=6.7$ (solid symbols) and $x=6.8$ (open symbols). Note that while the saturation value for the FM mode is larger for $x=6.7$, for both samples the MM peak optical bleaching is almost complete. The exponential decay fits (solid and dashed curves) are meant only as guides to the eye.

Of the four samples we have studied, only two possess chain fragments and display the related Raman modes. These two samples are compared in the inset of Fig. 1, normalized to the amplitude of the CuO_2-plane oxygen out-of-phase Raman-allowed mode at 330 cm^{-1}. The FM and MM modes are larger on the sample with oxygen composition $x=6.7$. This is consistent with nuclear quadrupole resonance experiments performed on $(Y,Gd)Ba_2Cu_3O_x$ as a function of oxygen composition, reported by Lütgemeier *et al.*[29] These clear experiments show a sharp increase of the mean chain length from about 10 to 30 when x goes from 6.7 to 6.8, together with a decrease of the number of (Raman-active) copper atoms with three-near-neighbor oxygens. Both features contribute to a reduction of the Raman signal due to the ''forbidden'' (end of fragment) modes. Interesting also is the compared photoexcitation dependence of the Raman peaks for $x=6.7$ and $x=6.8$, shown in Fig. 7(b). It turns out that while for both samples the bleaching of the ''monomer'' peak is almost complete, the saturation intensity of the FM peak is notably larger (around the double) for $x=6.7$. This is again consistent with our conclusion that photoexcitation acts mainly on the shortest (monomer) chain fragments, and that the latter almost disappear after prolonged illumination. The number of larger fragments is reduced mainly by the conjunction of two short ones into a larger one mediated by the jump of a monomer oxygen. It is expected that the residual Raman active fragments are less frequent in the sample with $x=6.8$ mainly because of two reasons: first, as we concluded above the number of short Raman active fragments is larger for $x=6.7$ due to the smaller mean chain length, and second, it is more likely that long chains become Raman silent after photoassisted conjunction if they start from larger fragments.

IV. CONCLUSION

We have presented Raman scattering experiments on oxygen deficient $GdBa_2Cu_3O_x$ thin films as a function of illumination and annealing induced oxygen disorder. Samples with oxygen content $x=6.53$, 6.7, 6.9, and 6.93 were studied. Raman lines unambiguously assigned to copper and oxygen vibrations involving atoms at the end of Cu-O chains were used as markers for the existence of short fragments. As a verification of this assignment, we find that these lines are observed only for the two samples with intermediate oxygen content, but not for $x=6.53$ and $x=6.93$. In the latter, the oxygen atoms in the basal plane are ordered forming infinitely long Cu-O chains in the so-called ortho-I and ortho-II structures. The dynamics of chain conjunction and fragmentation was monitored by the peak intensity dependences with photoexcitation time and annealing temperature. These results demonstrate the presence of photoassisted oxygen ordering in these high-T_c superconductors, and give definitive support for its ultimate role in the phenomena of persistent photoconductivity and photoinduced superconductivity.

Two Raman lines are observed in the spectral region corresponding to copper-atom vibrations at the end of chain fragments. We have proposed from a qualitative vibrational analysis the tentative assignment of the higher frequency one to a copper-mode in single oxygen Cu-O-Cu monomers, the other being due to larger chain fragments. We argue that this assignment is consistent with the observed photoexcitation induced narrowing of the assigned monomer Raman peak. The identification of these modes enabled us to conclude that photoassisted oxygen ordering occurs mainly through the reaccommodation of monomer oxygens, which results in the almost complete optical bleaching of the related Raman line. In contrast, a residual Raman signal due to copper vibrations at longer fragments persists after prolonged illumination. This saturation value can be related with the mean chain length, and thus depends on the oxygen content x of the sample. We believe that a proper description of the chain length distribution function, together with a bond polarizability model for the scattering by the vibrations of atoms at the end of chains, may provide quantitative information on the dynamics of chain formation and fragmentation with illumination and annealing.

ACKNOWLEDGMENTS

We would like to acknowledge fruitful discussions with B. Maiorov, G. Nieva, E. Osquiguil, and R. G. Pregliasco for invaluable help during different stages of the investigation. Special thanks are due to F. Tutzauer, R. Gludovats, C. Eggenschwiler, R. Soto, B. Eckardt, and G. Burmeister, for the construction and design of different parts of our experimental setup. The work was partially supported by Fundación Antorchas, Fundación Balseiro, and CONICET.

*Also at CONICET, Argentina.
[1] A. I. Kirilyuk, N. M. Kreines, and V. I. Kudinov, Pis'ma Zh. Éksp. Teor. Fiz. **52**, 696 (1990) [JETP Lett. **52**, 49 (1990)].
[2] G. Nieva, E. Osquiguil, J. Guimpel, M. Maenhoudt, B. Wuyts, Y. Bruynseraede, M. B. Maple, and I. K. Schuller, Phys. Rev. B **46**, 14 249 (1992); Appl. Phys. Lett. **60**, 2159 (1992).
[3] V. I. Kudinov, I. L. Chaplygin, A. I. Kirilyuk, N. M. Kreines, R. Laiho, E. Lähderanta, and C. Ayache, Phys. Rev. B **47**, 9017 (1993), and references therein.
[4] E. Osquiguil, M. Maenhoudt, B. Wuyts, Y. Bruynseraede, D. Lederman, and I. K. Schuller, Phys. Rev. B **49**, 3675 (1994).
[5] Y. H. Kim, C. M. Foster, A. J. Heeger, S. Cox, and G. Stucky, Phys. Rev. B **38**, 6478 (1988).
[6] J. F. Federici, D. Chew, B. Welker, W. Savin, J. Gutierrez-Solana, T. Fink, and W. Wilber, Phys. Rev. B **52**, 15 592 (1995).
[7] T. Endo, A. Hoffmann, J. Santamaria, and I. Schuller, Phys. Rev. B **54**, R3750 (1996).
[8] R. S. Decca, H. D. Drew, B. Maiorov, J. Guimpel, and E. Osquiguil, Appl. Phys. Lett. **73**, 120 (1998).
[9] V. I. Krylov, Pis'ma Zh. Éksp. Teor. Fiz. **52**, 1049 (1990) [JETP Lett. **52**, 442 (1990)].
[10] G. Uimin, Phys. Rev. B **50**, 9531 (1994), and references therein.
[11] V. G. Ivanov, M. N. Iliev, and C. Thomsen, Phys. Rev. B **52**, 13 652 (1995).
[12] C. Thomsen, in *Light Scattering in High-T_c Superconductors*, edited by M. Cardona and G. Güntherodt, Vol. 68 of Topics in Applied Physics (Springer, Berlin, 1991), pp. 285–359.
[13] C. Thomsen and M. Cardona, in *Physical Properties of High-Temperature Superconductors*, edited by D. M. Ginsberg (World Scientific, Singapore, 1989), Vol. I, p. 409.
[14] R. Liu, C. Thomsen, W. Kress, M. Cardona, B. Gegenheimer, F. W. de Wette, J. Prade, A. D. Kulkarni, and U. Schröder, Phys. Rev. B **37**, 7971 (1988).
[15] C. Thomsen, M. Cardona, B. Gegenheimer, R. Liu, and A. Simon, Phys. Rev. B **37**, 9860 (1988).
[16] E. T. Heyen, S. N. Rashkeev, I. I. Mazin, O. K. Andersen, R. Liu, M. Cardona, and O. Jepsen, Phys. Rev. Lett. **65**, 3048 (1990).
[17] E. T. Heyen, J. Kircher, and M. Cardona, Phys. Rev. B **45**, 3037 (1992).
[18] V. G. Hadjiev, C. Thomsen, J. Kircher, and M. Cardona, Phys. Rev. B **47**, 9148 (1993).
[19] M. Iliev, C. Thomsen, V. Hadjiev, and M. Cardona, Phys. Rev. B **47**, 12 341 (1993).
[20] D. R. Wake, F. Slakey, M. V. Klein, J. P. Rice, and D. M. Ginsberg, Phys. Rev. Lett. **67**, 3728 (1991).
[21] M. N. Iliev, H.-U. Habermeier, M. Cardona, V. G. Hadjiev, and R. Gajic, Physica C **279**, 63 (1997); M. N. Iliev, P. X. Zhang, H.-U. Habermeier, and M. Cardona, J. Alloys Compd. **251**, 99 (1997).
[22] O. Nakamura, E. E. Fullerton, J. Guimpel, and I. K. Schuller, Appl. Phys. Lett. **60**, 120 (1992).
[23] E. Osquiguil, M. Maenhoudt, B. Wuyts, and Y. Bruynseraede, Appl. Phys. Lett. **60**, 2159 (1992).
[24] J. Guimpel, B. Maiorov, E. Osquiguil, G. Nieva, and F. Pardo, Phys. Rev. B **56**, 3552 (1997).
[25] E. T. Heyen, R. Liu, C. Thomsen, R. Kremer, M. Cardona, J. Karpinski, E. Koldis, S. Rusiecki, Phys. Rev. B **41**, 11 058 (1990).
[26] M. Volkenstein, Dokl. Akad. Nauk SSSR **32**, 185 (1941); for a discussion on the transferability of bond polarizabilities and the application of the BPM to solids, see D. Bermejo, S. Montero, M. Cardona, and A. Muramatsu, Solid State Commun. **42**, 153 (1982).
[27] R. J. Cava, A. W. Hewat, E. A. Hewat, B. Batlogg, M. Marezio, K. M. Rabe, J. J. Krajewski, W. F. Peck, Jr., and L. W. Rupp, Jr., Physica C **165**, 419 (1990).
[28] B. Maiorov, Master Thesis, Instituto Balseiro, Comisión Nacional de Energía Atómica, 1997.
[29] H. Lütgemeier, S. Schmenn, P. Meuffels, O. Storz, R. Schöllhorn, Ch. Niedermayer, I. Heinmaa, and Yu. Baikov, Physica C **267**, 191 (1996).